Atmos. Meas. Tech. Discuss., 4, 527–562, 2011
www.atmos-meas-tech-discuss.net/4/527/2011/
doi:10.5194/amtd-4-527-2011

Atmospheric Measurement Techniques Discussions

Towards the improvement of cloud microphysical retrievals using simultaneous Doppler and polarimetric radar measurements

Y. Dufournet and H. W. J. Russchenberg

International Research Centre for Telecommunication and Radar (IRCTR), Delft University of Technology, Mekelweg 4, 2628 CD Delft, The Netherlands

Received: 30 September 2010 – Accepted: 13 December 2010 – Published: 21 January 2011

Correspondence to: Y. Dufournet (y.dufournet@tudelft.nl)

Published by Copernicus Publications on behalf of the European Geosciences Union.

Abstract

Radar-based retrievals are often employed to characterize the microphysical properties of cloud hydrometeors, i.e., their phases, habits, densities as well as their respective size and orientation distributions. These techniques are based on a synergetic use of different cloud observation sensor(s) and microphysical algorithm(s) where the information extracted from both sensors and models are combined and converted into microphysical cloud properties. However, the amount of available information is often limited, which forces current microphysical retrieval techniques to base their algorithms on several microphysical assumptions which affect the retrieval accuracy.

By simultaneously combining Doppler and polarimetric measurements obtained from fully Doppler polarimetric radar, it is possible to create spectral polarimetric parameters. Although these parameters are easily contaminated with unwanted echoes, this work shows that, from a correct radar signal processing based on filtering and averaging techniques, spectral polarimetric parameters can be correlated to microphysical cloud properties. In particular, preliminary results suggest that particle orientations and habits can be easily determined from the solely use of such spectral polarimetric parameters. Therefore, such additional microphysical information offers a great opportunity to improve current microphysical models by reducing their amount of microphysical assumptions.

1 Introduction

There is already a body of literature in atmospheric science considering cloud microphysical parameterizations as one of the main sources of error in operational climate and weather forecast models (e.g., Cantrell and Heymsfield, 2005; Kärcher and Koop, 2005). Microphysical processes deal with small spatial and time scales (smaller than a few centimeters and up to an hour) which are not directly resolved in global circulation models (GCM). Therefore, the parameterization of microphysical processes at GCM's resolution scale (up to 100 km and up to few hours) is based on

AMTD
4, 527–562, 2011

many assumptions which are currently not optimum at providing accurate description of the cloud microphysical state. Parameters governing the microphysical processes are cloud particle phases, their main orientations, their habits as well as their size distributions. A better understanding of such small scale processes and their characterization at large scale are of great importance in order to improve microphysical parameterizations. This can be achieved from the knowledge we gain from a proper use of cloud observation sensors (Shupe et al., 2008).

Radar sensors are commonly used to observe and retrieve microphysical properties within all types of cloud. A radiowave signal, transmitted from the radar through the atmosphere, is reflected by hydrometeors in a way that depends on the microphysical properties of the cloud. Thus, the backscattered signal (or better, the backscatter cross-section) contains microphysical information from the hydrometeors being probed at different ranges along the radar line of sight. Most microphysical retrievals are based on the computation of the Doppler spectrum of the radar signal, which is defined as the distribution of hydrometeors radial velocities weighted by the backscatter cross-section.

Typical radar-based retrievals only use the zero, first and second moments of the Doppler reflectivity spectrum, i.e., the reflectivity, the mean Doppler velocity and the Doppler width, respectively. However, these radar quantities contain information coming from a mixture of several microphysical parameters (as mentioned above) which are difficult to differentiate without the synergetic use of other sensors and microphysical model information. There are as many types of synergy as existing retrieval techniques. For example, the ice crystals size distribution and ice water content within ice clouds can be retrieved from dual-frequency techniques (Hogan et al., 1999) or from radar-lidar observation algorithms (Donovan et al., 2001). Several output uncertainties arise from such types of retrieval due to sensor calibration issues, assumptions in non-determined microphysical properties (such as particle habit and main orientation), simulation errors, and also microphysical inhomogeneity due to the large radar resolution volume being probed.

However, assuming a small vertical wind speed, it is possible to associate

AMTD
4, 527–562, 2011

particle fall velocities obtained by the radial velocity measurements with particle size distribution(s) of the cloud particle habit(s). Then, adding spectral information improves the identification and partitioning of cloud particles present within the same radar resolution volume (Shupe et al., 2003; Delanoe et al., 2006). Additionally, particle shape/orientation can be linked to the polarimetric information coming from the medium being probed (Russchenberg, 1992) when radars are equipped with polarimetric capability, which also enhances the microphysical characterization of cloud particles. In Matrosov et al. (2000), for example, polarimetric information is employed to infer the shape of cloud particles assuming spheroid shapes and microphysical homogeneity within the radar resolution volume. Notwithstanding their limitations, these finding suggest that Doppler and polarimetric information significantly improve cloud retrieval algorithms by reducing the number of microphysical assumptions.

In this paper, it is proposed to go a step further in cloud observation by building parameters which simultaneously combine both polarimetric and Doppler information contained in fully polarimetric radar signals, i.e., the spectral polarimetric parameters. It is believed that, based on these parameters, more cloud microphysical information can be obtained, reducing the number of assumptions employed in the previously mentioned cloud retrievals. The potential use of spectral polarimetric parameters within microphysical retrievals is therefore investigated in this paper. In the following section, spectral polarimetric parameters are defined and associated to microphysical cloud properties. Because the spectral polarimetric parameters are extremely noisy, the second half of this section describes how to process them so that they become statistically coherent in space and time for their use in microphysical retrieval techniques. An example of microphysical information retrievals using spectral polarimetry is tested in Sect. 3, on a retrieval algorithm focusing on ice/mixed-phase cloud microphysical properties (habits and orientations). In the same section, an illustration based on a case study is finally provided in order to demonstrate the potentiality of such a technique under mixed-phase cloud conditions. Finally, in Sect. 4, a summary of the retrieval technique and discussions are presented.

AMTD
4, 527–562, 2011

2 Spectral polarimetric parameters

This section describes how spectral polarimetric parameters are defined and processed in this work. Some illustrations are provided using spectral polarimetric measurements obtained with the S-Band TARA radar (Transportable Atmospheric Radar – Heijnen et al., 2000). Unlike most other atmospheric radars, TARA is based on the FM-CW principle. This technology provides better flexibility in terms of frequency modulation and sweep time (period of the frequency modulation), making the radar tunable for different spatial and time resolutions. TARA is composed of two large antennas, one continuously transmitting while the other continuously receives the backscattered signal. Both the transmitter and the receiver are equipped with polarizers that can change the polarization angle at either 0° or 90° (where 0° corresponds to an horizontal polarization state), as can be seen in Fig. 1. TARA is therefore classified as a Doppler fully polarimetric atmospheric radar profiler and can measure the different spectral polarimetric parameters mentioned in Sect. 2.1.

2.1 Definition and microphysical interpretation

The primary description of how the radar target backscatters the transmitted radar signal is given by the so-called scattering matrix **S** (Bringi and Chandrasekar, 2001). For radars equipped with linear polarization, **S** is defined such that,

$$\begin{bmatrix} E_h^r \\ E_v^r \end{bmatrix} = \frac{1}{r} \begin{bmatrix} \mathbf{S}_{hh} & \mathbf{S}_{hv} \\ \mathbf{S}_{vh} & \mathbf{S}_{vv} \end{bmatrix} \begin{bmatrix} E_h^i \\ E_v^i \end{bmatrix} = \frac{1}{r} \mathbf{S} \begin{bmatrix} E_h^i \\ E_v^i \end{bmatrix} \quad (1)$$

with $\overrightarrow{E}^s = E_h^r \hat{h}_r + E_v^r \hat{v}_r$ the scattered field in the linear basis $(\hat{h}_r, \hat{v}_r)$. For a reciprocal medium, $\mathbf{S}_{vh}$ equals $\mathbf{S}_{hv}$, which reduces the scattering matrix to three elements. Reciprocity property holds for meteorological targets and monostatic radars like TARA. The matrix elements can be obtained from any Doppler fully polarimetric atmospheric radar. From the Doppler information, the spectral scattering matrix elements, i.e.,

AMTD
4, 527–562, 2011

scattering matrix per Doppler bin, are also computed. Each spectral polarimetric parameter is derived from the spectral scattering elements and related to specific cloud properties.

The spectral horizontal/vertical reflectivity parameter sZ_{XX} (XX referring to either vertical or horizontal polarization state) is expressed as,

$$sZ_{XX}(v) = \langle S_{XX}(v) S^*_{XX}(v) \rangle \tag{2}$$

where $\langle\,\rangle$ denotes the time average of the Doppler spectra. In particular, this parameter is related to the particle size distribution of the medium being probed.

The spectral differential reflectivity ratio $sZ_{DR}(v)$ is defined as the ratio between the two copolar signals, $sZ_{HH}(v)$ and $sZ_{VV}(v)$, such that,

$$sZ_{DR}(v) = \frac{sZ_{HH}(v)}{sZ_{VV}(v)} = \frac{\langle S_{HH}(v) S^*_{HH}(v) \rangle}{\langle S_{VV}(v) S^*_{VV}(v) \rangle} \tag{3}$$

This parameter has as its main advantage that it is independent from any absolute radar calibration. It is, above all, linked to the shape and orientation of the hydrometeors, i.e., their axis ratio assuming spheroid shapes. Optimum sZ_{DR} measurements are obtained at a 45° elevation angle in order to benefit from both, the polarization diversity measurements from non-spherical hydrometeors, and the falling particle velocity information obtained from the Doppler measurements. However, $sZ_{DR}(v)$ can have very low values when used in radar profiling techniques, and is still strongly affected by unwanted echoes.

The ratio between the cross-polar and the co-polar spectral reflectivity is called the linear depolarization ratio $sL_{DR,x}(v)$, x being either the vertical or horizontal polarization state of the copolar reflectivity signal,

$$sL_{DR,x}(v) = \frac{sZ_{HV}(v)}{sZ_{xx}(v)} = \frac{\langle S_{HV}(v) S^*_{HV}(v) \rangle}{\langle S_{xx}(v) S^*_{xx}(v) \rangle} \tag{4}$$

AMTD
4, 527–562, 2011

$sL_{\mathrm{DR},x}(v)$ is mainly related to the tumbling effect of the falling cloud particles. However, note that this parameter has also been used to characterize particle habits within ice clouds (Matrosov et al., 2000).

The last spectral parameter, the spectral complex copolar cross-correlation coefficient $s\rho_{\mathrm{co}}(v)$, is defined as,

$$s\rho_{\mathrm{co}}(v) = \frac{\langle S_{\mathrm{HH}}(v) S^{*}_{\mathrm{VV}}(v) \rangle}{\sqrt{\langle |S_{\mathrm{HH}}|^2 \rangle \langle |S_{\mathrm{VV}}|^2 \rangle}} \tag{5}$$

As shown in Eq. (2.5), the spectral complex copolar cross-correlation coefficient is associated to the correlation between HH and VV spectra. Battaglia et al. (2001) demonstrated that $\rho_{\mathrm{co}}(v)$ (and therefore $s\rho_{\mathrm{co}}(v)$) is sensitive to the particle habit as for $sL_{\mathrm{DR},x}(v)$.

2.2 Spectral polarimetric processing within ice/mixed-phase clouds

As displayed in Fig. 2, spectral polarimetric parameters are, by definition, represented as a vector instead of a single scalar as with any other standard radar parameters. They are, therefore, statistically much more unstable and require specific processing in order to use them within cloud microphysical retrieval techniques. The radar signal coming from the TARA receiver can be depicted as a mixture of wanted received echoes (from meteorological targets), unwanted echoes (clutter), and noise. Direct filtering steps are first applied on the spectral polarimetric signal in order to remove noise and unwanted echoes, as listed below:

2.2.1 Smoothing

The Doppler spectra computed from the raw signal are very noisy (see Fig. 3a), which make them difficult to study. The signal is first smoothed in order to remove most of the statistical variations while keeping the main slope of each spectrum (see Fig. 3a).

AMTD
4, 527–562, 2011

2.2.2 Correction for spectral aliasing and non-simultaneous polarimetric measurements

For the TARA radar, a sequence of measurements at different polarization settings is used in order to obtain all the spectral scattering matrix elements. Increasing this sequence consequently reduces the maximum unambiguous velocity of the radar. For some atmospheric situations with strong convection, this can lead to Doppler spectrum aliasing. Moreover, the target's dynamical properties also affect the polarimetric accuracy of the radar data because of the non-simultaneity of the measurements carried out at different polarization settings. The data are, therefore, corrected for spectrum aliasing and non-simultaneous polarimetric measurement using Unal and Moisseev (2004). A consequence of this correction is also the reduction of noise and clutter. Such unwanted echoes are indeed reallocated to a different Doppler velocity window than the one where meteorological echoes are present (as can be seen on Fig. 3b for the signal present below $-8\,\mathrm{m\,s^{-1}}$ or above $+8\,\mathrm{m\,s^{-1}}$).

2.2.3 Double sL_{DR} clipping

The clipping is based on the work by Unal (2009). A double filtering technique is applied in the spectral linear depolarization ratios, $sL_{\mathrm{DR},H}$ and $sL_{\mathrm{DR},V}$. For both, a clipping above $-5\,\mathrm{dB}$ is performed and values above this threshold are considered as non-meteorological echoes. From this clipping, only the Doppler velocity window containing meteorological echoes is kept. Figure 3c shows an example of the sZ_{VV} spectra obtained after the implementation of the double sL_{DR} clipping. In that specific case, the velocity window has been constrained between about -4 and $-1\,\mathrm{m\,s^{-1}}$.

2.2.4 Additional processing

Among all the spectral polarimetric parameters, $sZ_{\mathrm{DR}}(v)$ is the most affected by unwanted echoes. This is mainly due to its low values (in the order of tenth of a dB),

AMTD
4, 527–562, 2011

which are within the same order of magnitude as the radar accuracy. After applying all the processing steps mentioned in Sects. 2.2.1–2.2.3, $sZ_{DR}(v)$ still remains affected by strong signal fluctuations. In order to improve microphysical retrieval techniques based on spectral polarimetric parameters, some further filtering can be applied using additional clipping and statistical estimators computed from $sZ_{DR}(v)$. It has to be pointed out that these additional steps are only performed in case of high reflectivity values, above 0 dB, in order to ensure high signal-to-noise ratio:

2.2.5 Additional clipping

The threshold values obtained for this additional clipping are obtained from a sensitivity analysis performed on the spectral polarimetric parameters. This analysis was carried out over a set of different ice/mixed-phase cloud probed with the TARA radar. It was found that, within ice cloud systems (precipitation and ice/mixed-phase clouds), the clipping on $sL_{DR,H}$ and $sL_{DR,V}$ could be leveled up to −15 dB without affecting the meteorological echoes.

Furthermore, using $sZ_{DR}(v)$ within microphysical retrievals implies a very high correlation between the Doppler spectra obtained in HH and VV polarization states. It was demonstrated that the remaining noise and clutter still present in the signal could be removed by an additional clipping based on spectral polarimetric correlation, using the spectral copolar cross-correlation coefficient $s\rho_{co}(v)$. Within ice clouds, Battaglia et al. (2001) simulated different polarimetric parameters for different ice particle habits and radar elevations. At 45° elevation angle (standard TARA working elevation when working with spectral polarimetry – see Sect. 2.1), typical ρ_{co} values above 0.9 could be simulated. In this work, the clipping is performed on the spectral mode at $s\rho_{co}(v)$=0.94 in order to discard the remaining noise echoes.

Nevertheless, the dealiasing technique can produce an overestimation of $s\rho_{co}(v)$ in the remaining noise data region inherent of the cross-correlation computation (Eq. 2.5). This is not the case when looking at the variation of $s\rho_{co}(v)$ on consecutive Doppler bins, i.e., $\Delta s\rho_{co}(v)$. Thus, a third filtering is applied in parallel on $\Delta s\rho_{co}(v)$, values

AMTD
4, 527–562, 2011

above 0.01 being removed from the spectra. In conclusion, only the Doppler part of the spectrum satisfying the three thresholds on $sL_{DR,X}(v)$, $s\rho_{co}(v)$ and $\Delta s\rho_{co}(v)$ is kept. An example of such additional clipping is provided in Fig. 4. For this specific example, the Doppler velocity window was further constrained from −3.8 to −2.7 m s^{-1}.

2.2.6 Additional averaging

The single use of an additional Doppler velocity clipping does not remove the statistical variations present in the sZ_{DR} Doppler region where meteorological are present. These fluctuations arise from the dynamical and microphysical inhomogeneities of the atmosphere. Such variations can produce incoherent behavior of consecutive spectra in time if the Doppler spectra are not averaged. By averaging over time a number N_{av} of initial non-averaged sZ_{DR} spectra, it is possible to remove statistical variations. At each range and time bins, the number of initial spectra to average (corresponding to a specific the averaging time) is determined. It is based on a statistical analysis of the sZ_{DR} slope, i.e., the main trend of the sZ_{DR} spectrum, performed on a set of sZ_{DR} spectra averaged over an increased time amount. The main trend of each spectrum is obtained from a second order polynomial fit in order to reduce the second order fluctuation of the signal. For the analysis, a set of 15 spectra is created at each time and range bins of the reflectivity profile. Each spectrum is averaged with an increasing number of initial spectra obtained at 1.5 s intervals, i.e., with an increasing averaging time. For the sake of clarity, the spectrum 1 (N_{av}=1) is not averaged (initial 1.5 s resolution) and the spectrum 15 (N_{av}=15) is averaged with the following 15 initial spectra, corresponding to a maximum time amount of 23 s. An example is given in Fig. 5 for spectra obtained at different consecutive time bins, before (middle row) and after (bottom row) averaging on a specific time amount (specific N_{av} value) determined from the statistical analysis. Each spectrum from left to right is obtained within an ice cloud event and at 1.5 s interval. The main slope of each spectrum is determined from its parabolic fit. The noticeable difference in the parabolic fit of both Doppler spectra, before and after averaging, is analyzed from two different statistical parameters, the

AMTD
4, 527–562, 2011

standard deviation "std" and the correlation factor "R_d", described below:

– The standard deviation std: the parabolic fit is first used to compute the standard deviation at each averaging step,

$$\mathrm{std} = \frac{\sqrt{\frac{1}{M}\sum_{v\min}^{v\max}\left|sZ_{VV}(v) - sZ_{VV}^{fit}(v)\right|^2}}{\sqrt{\frac{1}{M}\sum_{v\min}^{v\max}\left|\frac{sZ_{VV}(v)+sZ_{VV}^{fit}(v)}{2}\right|^2}} \quad (6)$$

where M corresponds to the total number of Doppler velocity bins and sZ_{VV}^{fit} is the parabolic fit of the sZ_{VV} spectra. "Std" is related to the amplitude of the sZ_{DR} fluctuations. An example of the "std" evolution for an increasing averaging time is provided in Fig. 6b together with the gradient of "std". Within clouds, the variation of "std" over an increasing averaging time can be linked to the particle shift to neighboring Doppler bins due to the presence of micro-turbulence within the same resolution volume. Because of the randomness of the Doppler shifts, the standard deviation of the signal usually decreases as the time averaging increases as shown in Fig. 6b. As previously mentioned, the slope of "std" (i.e., its gradient) is also monitored, low fluctuations of the slope ensuring a minimum homogeneity of the signal over time. In this work a minimum number of averaging spectra $N_{av,min}$ (corresponding to a minimum averaging time) is determined when both, the *std* coefficient and its gradient become lower than 0.15 and 0.015, respectively, corresponding to the polarimetric accuracy of the TARA radar. $N_{av,min}$ is equal to 5 in the example displayed in Fig. 6.

– Correlation factor R_d: when averaging over a time period longer than $N_{av,min}$ (i.e., over a high number of spectra N_{av}), some multi-modal signals with coherent maxima at specific Doppler bins can occur. Beside, Doppler shift and spectral

AMTD
4, 527–562, 2011

broadening of the full Doppler spectra can also appear when averaging over a time period longer than 23 s (>15 spectra averaged), as shown in Fig. 7. These stationary spectral processes over time are related to real microphysical or dynamical variations within the cloud being probed which can occur in less than a few seconds. They are not strongly affecting the "std" analysis but they can drastically change the sZ_{DR} slope, and therefore, the coherency of two consecutive Doppler spectra. The correlation factor R_d is computed in order to monitor the spectral coherency of the parabolic fit over time:

$$R_d = \frac{\sum_v \left(sZ^{fit}_{DR,N_{av,min}}(v) - \left\langle sZ^{fit}_{DR,N_{av,min}} \right\rangle\right)\left(sZ^{fit}_{DR,N_{av}}(v) - \left\langle sZ^{fit}_{DR,N_{av}}(v)\right\rangle\right)}{\sqrt{\sum_v \left(sZ^{fit}_{DR,N_{av,min}}(v) - \left\langle sZ^{fit}_{DR,N_{av,min}} \right\rangle\right)^2 \left(sZ^{fit}_{DR,N_{av}}(v) - \left\langle sZ^{fit}_{DR,N_{av}}(v)\right\rangle\right)^2}} \quad (7)$$

As can be seen in Eq. (2.7), the spectra obtained from the average of $N_{av,min}$ initial spectra is taken as reference. R_d is expressed in percent, and is equal to 100% for two identical spectra, i.e., 100% correlation. Figure 6c displays the correlation evolution of R_d as well as its gradient. For a reliable microphysical retrieval, high coherency within nearby averaged spectra should be observed. This guarantees that measurements are performed within a homogeneous resolution volume in terms of microphysical and meso-scale dynamical cloud properties. Some previous work (Dufournet, 2010), showed that a 10% decorrelation of the sZ_{DR} signal could strongly affect the output of the microphysical technique, and mainly the concentration of oriented ice particles. A 10% threshold is also adopted within this paper. An averaged spectra having showing more than 10% decorrelation will be discarded. In the example taken in Fig. 6c, all spectra averaged with N_{av} greater than 12 (averaging time above 18 s) are not considered coherent and cannot be averaged together with the previous initial spectra.

AMTD
4, 527–562, 2011

At this stage of the processing, a final averaging time (or number N_{av} of initial spectra to average) can be obtained. It corresponds to the minimum averaging time where all the three thresholds mentioned above (i.e., on "std" and its gradient, and R_d) are satisfied. In Fig. 6, for example, an averaging of at least 5 initial Doppler spectra, corresponding to an averaging time of 7.6 s, is chosen in order to remove any microphysical and dynamical fluctuation in the Doppler signal.

3 Application for ice cloud microphysical retrievals

To further support the potential of using spectral polarimetric parameters, a method is presented in this section where particle habit(s) and orientation(s) are retrieved from the TARA radar within ice/mixed-phase clouds. It is important to note that this method is still in a preliminary stage and is therefore only described in order to illustrate the potential of using the spectral polarimetric parameters in the microphysical retrievals. At the TARA working frequency of 3.3 GHz, only cloud ice crystals and falling drops (drizzle and rainfall) are detected within the measurements, cloud water and supercooled water droplets being too small (mean size of about 20 µm) to be discerned by the radar. If we assume that most ice crystals grow rapidly to a recognizable non-spherical shape larger than 25 µm due to high supersaturation with respect to ice (Lawson et al., 2001), TARA can be used to provide direct ice crystal observations without being affected by the supercooled water phase in mixed-phase cloud regions.

The microphysical algorithm is based on different spectral and integrated polarimetric parameters, that is, $sZ_{DR}(v)$, $s\rho_{co}(v)$ and L_{DR}. The retrieval follows the below-mentioned steps:

3.1 Partitioning of cloud particle type

As previously mentioned, most radar resolution volumes can contain different hydrometeor types which evolve within the same cloud bulk. The probability of particle

AMTD
4, 527–562, 2011

mixing is even more important at a far distance from the radar as the radar volume expands when this distance increases. Most current retrieval outputs assume the microphysical homogeneity of the medium being retrieved. Thus, cloud particle mixing can lead to wrong characterization of parameters such as the particle density, shape and phase which, in turn, affect the microphysical retrieval outputs.

Hydrometeors detected in each radar cell are spectrally classified into different groups based on the similarity of their size, shape and main orientation. Because $sZ_{DR}(v)$ is related to such microphysical parameters (see Sect. 2.1), the algorithm uses the variations detected in the slope of $sZ_{DR}(v)$ over the whole spectrum in order to infer the changes within the particles properties. The particle classification is facilitated by applying a parabolic fit on $sZ_{DR}(v)$ beforehand so that the second order fluctuations of the original spectrum are discarded. Within a set of cloud observations performed with TARA, 16 main particle arrangements, each comprising 1 to 3 groups of particles, have been defined from the main slope of the sZ_{DR} spectrum, as displayed in Fig. 7. A categorization number N_{cat} is attributed to each radar cell retrieved. For the sake of clarity, a schematic representation of the microphysical ice crystal's characteristics is added on the left hand panel of Fig. 7.

3.2 Characterization of ice crystal orientation

Ice crystal orientation is caused by the airflow passing around the particle. This airflow creates low pressure at the crystal edges resulting in a torque which tends to align the axis of symmetry of the particle along the airflow's direction (Brussaard, 1976). However, different dynamical mechanisms such as windshear or strong updraft can act upon the airflow's orientation, changing the particle's orientation. Crystal orientations play a role in the particle fall velocity computation (Mitchell et al., 1996), which is often used for the determination of the particle size distribution. A good estimation of the ice crystal's orientation is therefore required.

At the TARA wavelength (≈10 cm), the ice particle's orientation can be directly obtained from the mean sZ_{DR} value(s) measured for each group of particles detected

AMTD
4, 527–562, 2011

in the same resolution volume. A fairly simple orientation algorithm is currently implemented in the microphysical retrieval. Each ice crystal species is assumed to be composed of either horizontally, vertically or randomly oriented particles. For a Doppler spectrum region (related to a specific group of ice crystals) with positive $sZ_{DR}(v)$, the predominant ice particles are assumed to be horizontally aligned. This is the case for some ice crystal groups detected in radar volumes with N_{cat} above 10. Conversely, negative $sZ_{DR}(v)$ are related to predominant vertically oriented ice crystals ($0<N_{cat}<9$). Ice crystals present in Doppler regions where $sZ_{DR}(v)$ is close to zero show properties similar to spherical particles. In terms of orientation, $sZ_{DR}(v)=0$ can be interpreted as particles having random orientations. Such random orientations can be caused by the different aerodynamic effects affecting the different particle shape. Besides, turbulence effects are also responsible for random particle orientation when large sZ_{DR} fluctuations around zero are observed all over the spectrum (for $N_{cat}=0$).

3.3 Characterization of ice crystal habit

More than 60 ice crystal species have been observed within natural clouds (Mogano and Lee, 1966). However, this classification can be simplified by merging particle habits into four categories while still keeping a fairly good approximation of the particle shape: pristine ice crystals (comprising plate, dendrite and column and needle-like ice crystals), aggregate, graupel and hail. As for the orientation, particle habits also affect most of the microphysical retrievals, a wrong shape assumption leading to wrong particle density, wrong axis ratio (if ice crystal shapes is assumed spheroidal), and wrong fall velocity computations.

The presented particle habit retrieval technique is meant to work within mixed-phase cloud having low riming processes. Under such a condition, a simple categorization scheme can be employed, partitioning the particle into the three following groups: aggregates, plate-like and column-like ice crystals. Again, different spectral polarimetric tools are used for the shape/habit categorization. The spectral cross-correlation parameter is first investigated in order to distinguish the aggregates

AMTD
4, 527–562, 2011

from the pristine ice crystals. High $s\rho_{co}$ values, above 0.995, are observed when aggregates predominate the full radar resolution volume (i.e., as assumed in this paper for N_{cat}=0). Conversely, smaller ρ_{co} values can be simulated from different pristine ice crystals when the radar antennas are titled at 45° elevation angle. Because mixing different particle types affect the $s\rho_{co}$ distribution, a weighting factor R_w is created for the particle habit categorization and defined so that,

$$R_w = \frac{\sum_{i=0.995}^{i=1} N_i}{\sum_{i=0.95}^{i=0.97} N_i} \quad (8)$$

where N_i is the total number of spectral samples per bin i. This R_w ratio is preferred rather than using the mean or the standard deviation of the distribution, $s\rho_{co}$ values being too small to use standard statistical tools. When R_w<2 (threshold determined empirically), it is assumed that pristine ice crystals dominate the radar resolution volume. Aggregates dominate in the other cases.

Secondly, the type of pristine ice crystals (plate- or column-like ice crystals) was investigated from the combination of R_w with the linear depolarization ratio L_{DR}. As mentioned in Sect. 2.1, L_{DR} strongly depends on the axis ratio and canting angle of the particles. L_{DR} increases when increasing the standard deviation of the canting angle from all hydrometeors, i.e., passing from perfectly to randomly oriented ice crystals. As a result, significant differences in L_{DR} between plate- and column-like crystals are expected when a non-random orientation is considered, according to Battaglia et al. (2001). For the categorization algorithm, a first threshold guess was employed to distinguish plate from column within pristine ice regions. At 45° elevation angle, simulated L_{DR} distribution, centered around −15 dB, suggested the presence of columns whereas L_{DR} was mostly below −20 dB for plate-like ice crystals. A summary of the crystal habit categorization is provided in Table 1.

AMTD
4, 527–562, 2011

3.4 Case study of 21 July 2007

During summer 2007, the TARA radar took part in the Convective and Orographically-induced Precipitation Study (COPS) with the aim of studying heavy precipitation events driven by orographic conditions at high resolution scales. Precipitation processes were observed by means of a synergetic collection of research remote-sensing and/or in-situ systems operated at the ground, on-board aircrafts and satellites. Six main ground-based sites (site P, R, H, M, S and V) were deployed across the COPS domain (see Fig. 9). More information on the campaign can be found in Wulfmeyer et al. (2008). TARA was located on the H site (Hornisgrinde), on top of a plateau, close to other ground-based sensors. In this paper, Saturday, 21 July 2007, is taken as a case study in order to illustrate the microphysical approach described in the previous section.

During that day, a frontal zone was affecting the COPS area with cold air in the north and warm air in the south. A wave (with the presence of high pressure ridge) was developing and stretching southwest to northeast up to the COPS domain, leading to the formation of a low pressure area over Bavaria. This system was responsible for upward vertical motion and the formation of a Mesoscale Convective System (MSC) moving northeastwards over the eastern half of the COPS area in the course of the afternoon. In terms of cloud coverage, widespread clouds, turning to convective (enhanced by the orography) and rainy cells in the afternoon were observed. TARA measured in the afternoon to sample the MCS over the COPS domain. The TARA measurements were combined with synchronous aircraft in-situ measurements performed with the ATR42 aircraft from Safire, in the frame of the OSMOC project (Observation Strategy for Mixed-phase Orographic Clouds) under the umbrella of EUFAR activities (European Fleet for Airborne Research).

3.4.1 TARA measurements and interpretation

TARA started to measure from 13:05 UTC at 45° elevation angle. Figure 10a shows the reflectivity profile obtained from 15:45 UTC onwards during that day. The MSC

AMTD
4, 527–562, 2011

captured from 16:20 to 16:45 UTC was taken as case study for the microphysical retrieval. During this time slot, a cloud with great vertical extension from 3200 m to 6400 m (nimbostratus type) was observed. Because of the high reflectivity encountered in this mid-level cloud region (above 10 dBZ), ice crystals were very likely present. Just below 3200 m, a bright band was detected indicating the melting of the precipitating ice crystals. Quite heavy precipitation resulted from such a melting process, with reflectivity values reaching 40 dBZ. From a dynamical point of view, analyses of the mean Doppler velocity and Doppler width profiles revealed the presence of a strong updraft (Dufournet, 2010) probably enhanced by an orographic effect acting on a westerly wind flow, which could play a role on particle orientation.

3.4.2 Microphysical retrieval results

The microphysical retrieval technique was tested on the ice/mixed-phase cloud passing over the H site from 16:20 to 16:45 UTC, where high signal to noise ratio was detected.

The black box in Fig. 10a bounds the retrieval area. The results of the retrievals are then displayed in Fig. 10b–e. The mapping of the partitioning and orientation categorization procedures, explained in Sects. 3.1 and 3.2, is represented in Fig. 10b using a simplified color scale. Some of the categorization numbers N_{cat} defined in Fig. 8 are merged with respect to the particle orientation(s) and number of species present within each radar resolution volume. On the one hand, light yellow pixels, grouping N_{cat}=12, 14 or 16 (radar volume containing up to 2 cloud particle types) and N_{cat}=11, 13 or 15 (radar volume containing at least 2 cloud particle types), represent cloud bulks where at least one particle type is horizontally aligned. On the other hand, N_{cat}=3, 5 or 7 and N_{cat}=4, 5 or 8 represent vertically aligned cloud particles. Aggregates are considered to be present within each radar cell. Still, a specific color scale for N_{cat}=0 is defined when it is assumed that only randomly oriented aggregates fill the resolution volume. Oriented particles were often detected in this cloud. A change of orientation with time was also observed around 16:30 UTC. This discrepancy was closely linked to a change in the Doppler width coefficient, which could arise from

AMTD
4, 527–562, 2011

a strong variation of the amplitude of the horizontal wind, leading to production of turbulence and changes in the ice crystal orientation.

Looking at the relative proportion between oriented and randomly oriented particles, it was noticed that oriented particles (mainly horizontal alignment) were much more represented at cloud top. This trend was reversed as reaching cloud bottom. Figure 10c maps the weighting coefficient defined in Sect. 3.3. Because R_w was low at cloud top, oriented particle found in this region were certainly pristine ice particles. Combining this information with the mean of the L_{DR} distribution found for the same cloud region ($L_{DR} \approx -21$ dB as seen in Fig. 10d), horizontally plate-like particles were most probably produced at cloud top. As we go further down, R_w increased suggesting the occurrence of ice crystal aggregation processes. Even some strong aggregation areas at cloud bottom, with $R_w > 4$, were observed. This result is shown in the simplified categorization of Fig. 10e. From this figure, good agreement was found between the cloud processes and the precipitation regime observed below the melting layer, e.g., strong aggregation areas connected to heavy rainfall regimes as explained in Dufournet (2010).

3.4.3 Ice crystal habit assessment using the COPS facilities

An ATR42 flight was coordinated the very same day with the TARA measurements in the frame of the OSMOC project, taking advantage of the COPS facilities, i.e., a specific daily weather forecast dedicated to the COPS area coupled with a dense measurement network providing a detailed nowcasting of the cloud overcast. This aircraft is an ATR42-320 aircraft modified for scientific use, and has flying performances suitable for the study of ice/mixed-phase clouds in complex terrain. In order to satisfy the need of the OSMOC experiment, an aircraft configuration focused on microphysical measurements was adopted. For the particle habit assessment, the 2D-C probe images obtained during in-cloud penetrations were analyzed at different flight levels (Fig. 11a). Plate and dendrites, mixed with small aggregate particles, were mainly found at cloud top (about 5000 m altitude). For flight legs performed at lower

AMTD
4, 527–562, 2011

altitude, only aggregates at different riming stages were observed. This result is in good agreement with the retrieved ice particles habits obtained from TARA spectral polarimetric parameters. It can be noticed that graupels were also observed within a high riming region, but their retrievals were not implemented in the algorithm yet.

Finally, the plate-like type of pristine ice was also confirmed when looking at the radiosonde launch of the M site. From Fig. 11b, cloud temperatures below −10 °C were found at cloud top, which is favorable for plate-like crystal formation according to Lamb and Scott (1972).

4 Conclusions

Most cloud microphysical retrieval techniques suffer from a lack of microphysical information provided by current observation, such as radar sensors, for the microphysical characterization of ice/mixed-phase clouds. Several assumptions are required to fill this lack, which strongly affects the retrieval accuracy needed for a correct and complete cloud microphysical description, such as assumption in particle density, orientation and particle types within the same cloud bulk (Donovan et al., 2005; Matrosov et al., 2000). In this paper, we have investigated the use of simultaneous Doppler and polarimetric radar measurements within ice/mixed-phase clouds for microphysical retrievals. It has been shown that a tight relation exists between spectral polarimetric parameters and the cloud microphysical properties, providing a wealth of additional microphysical information from a single radar signal, which reduces the cloud microphysical retrieval uncertainties.

Several spectral polarimetric data obtained from the TARA radar have been analyzed. Because spectral polarimetric parameters are by nature extremely noisy, this analysis has mainly concentrated on how to process them. This work strongly argues that the correct choice of a specific signal filtering method combined with an adequate time averaging is of great importance to ensure the spatial and temporal coherency of the spectral polarimetric parameters, and thereby, consistent spatial and temporal microphysical retrieval outputs.

AMTD
4, 527–562, 2011

In the second half of the paper, simple retrieval microphysical algorithms (number of ice crystal species, main particle orientations and habits) were defined and applied to TARA measurements carried out during the COPS campaign on 21 July 2007. The retrieval outputs were found to be consistent with collocated measurements performed on site or on-board the ATR42 aircraft on the very same day, which is encouraging for further investigations. Despite its preliminary character, the research reported here would seem to indicate that, already with simple retrieval techniques, spectral polarimetry can provide additional microphysical information, not often taken into account in current retrievals, i.e., the number of ice crystal species present in each cloud resolution volume and their main orientation.

The use of retrievals based on spectral polarimetric parameters is likely to be a fruitful area of further work. On the one hand, the simple retrievals defined in Sect. 3 can be improved for operational use. Also new retrieval algorithms based on spectral polarimetric parameters are currently investigated for the characterization of the particle size distribution within ice/mixed-phase clouds. On the other hand, the achieved results could already be implemented within current retrieval algorithms in order to reduce the number of assumptions used. For example, the ice crystal density, considered to be critical in radar-lidar methods (Delanoe et al., 2006), could better be characterized from the particle habits retrieved from spectral polarimetric measurements.

Acknowledgements. The authors wish to thanks the crew of the ATR42 aircraft as well as the EUFAR organization, as well as the Lamp institute (Laboratoire de Meteorologie Physique – Clermont-Ferrand, France) which provided the necessary processed in-situ data. The authors also wish to thanks the COPS organization committee for the help in achieving the collocated measurements during the campaign.

AMTD
4, 527–562, 2011

References

Battaglia, A., Sturniolo, O., and Prodi, F.: Analysis of polarization radar returns from ice clouds, Atmos. Res., 59–60, 231–250, 2001.

Bringi, V. and Chandrasekar, V.: Polarimetric Doppler Weather Radar – Principle and applications, Cambridge University Press, UK, 2001.

Brussaard, G.: A meteorological model for rain induced crosspolarization, IEEE Trans. AP, USA, 24, 5–11, 1976.

Cantrell, W. and Heymsfield, A.: Production of ice in tropospheric clouds – a review, B. Am. Meteorol. Soc., 86(6), 795–807, 2005.

Delanoe, J., Protat, A., Bouniol, D., Heymsfield, A., Bansemer, A., and Brown, P.: The characterization of ice cloud properties from Doppler radar measurements, J. Appl. Meteorol. Climatol., 46, 1682–1698, 2006.

Donovan, D. and Lammeren, A.: Cloud effective particle size and water content profile retrievals using combined lidar and radar observations 1. theory and examples, J. Geophys. Res., 106, 27425–27448, 2001.

Dufournet, Y.: Ice crystal properties retrieval using radar spectral polarimetric measurements within ice/mixed-phase clouds, Ph.D. thesis, Technische Universiteit Delft, 2010.

Heijnen, S., Ligthart, L., and Russchenberg, H.: First measurements with TARA; an S-band transportable atmospheric radar, Phys. Chem. Earth B, 25, 995–998, 2000.

Hogan, R. J., Illingworth, J., and Sauvageot, H.: Measuring cystal size using 35- and 94-GHz radars, J. Atmos. Ocean. Tech., 17, 27–37, 1999.

Kärcher, B. and Koop, T.: The role of organic aerosols in homogeneous ice formation, Atmos. Chem. Phys., 5, 703–714, doi:10.5194/acp-5-703-2005, 2005.

Lamb, D. and Scott, W.: Linear growth rates of ice crystals grown from the vapor phase, J. Cryst. Growth, 12, 21–31, 1972.

Lawson, R., Baker, B., Schnitt, C., and Jensen, T.: An overview of microphysical properties of arctic clouds observed in May and July 1998 during fire ace, J. Geophys. Res., 106, 14989–15014, 2001.

Matrosov, S. Y., Reinking, R. F., Kropfli, R. A., Martner, B. E., and Bartram, B. W.: On the use of radar depolarization ratios for estimating shapes of ice hydrometeors in winter clouds, J. Appl. Meteorol., 40, 479–490, 2000.

AMTD
4, 527–562, 2011

Mitchell, D.: Use of mass- and area-dimensional power laws for determining precipitation particle terminal velocities, J. Atmos. Sci., 53, 1710–1723, 1996.
Mogano, C. and Lee, C.: Meteorological classification of natural snow crystals, J. Fac. Sci., 2, 321–335, 1966.
Russchenberg, H.: Ground-based remote-sensing of precipitation using a multi-polarized FM-CW Doppler radar, Ph.D. thesis, Technische Universiteit Delft, 1992.
Shupe, M. D., Kollias, P., Matrosov, S. Y., and Schneider, T. L.: Deriving mixed-phase cloud properties from Doppler radar spectra, J. Atmos. Ocean. Tech., 21, 660–670, 2003.
Shupe, M. D., Daniel, J., de Boer, G., Eloranta, E., Kollias, P., Long, C., Luke, E., Turner, D., and Verlinde, J.: A focus on mixed-phase clouds: the status of ground-based observation methods, B. Am. Meteorol. Soc., 89, 1549–1562, 2008.
Unal, C. M. H.: Spectral polarimetric radar clutter suppression to enhance atmospheric echoes, J. Atmos. Ocean. Tech., 26, 1781–1797, 2009.
Unal, C. M. H. and Moisseev, D.: Combined Doppler and polarimetric radar measurements: correction for spectrum aliasing and nonsimultaneous polarimetric measurements, J. Atmos. Ocean. Tech., 21, 443–455, 2004.
Wulfmeyer, V., Behrendt, A., Bauer, H.-S., Kottmeier, C., Corsmeier, U., Blyth, A., Craig, G., Schumann, U., Hagen, M., Crewell, S., Di Girolamo, P., Flamant, C., Miller, M., Montani, A., Mobbs, S., Richard, E., Rotach, M. W., Arpagaus, M., and Russchenberg, H.: The convective and orographically-induced precipitation study: a research and development project of the World Weather Research Program for improving quantitative precipitation forecasting in low-mountain regions, B. Am. Meteor. Soc., 89(10), 1477–1486, 2008.

AMTD
4, 527–562, 2011

Table 1. Crystal habit categorization.

Ice particle type present in the resolution volume	Categorization parameters
Aggregates dominating the Doppler spectra	$N_{cat}=0$ and/or $R_w \gg 2$
Column-like crystals dominating the Doppler spectra	$R_w<2$ and $L_{DR}\approx -15$ dB
Plate-like crystals dominating the Doppler spectra	$R_w<2$ and $L_{DR}\approx -20$ dB

AMTD
4, 527–562, 2011

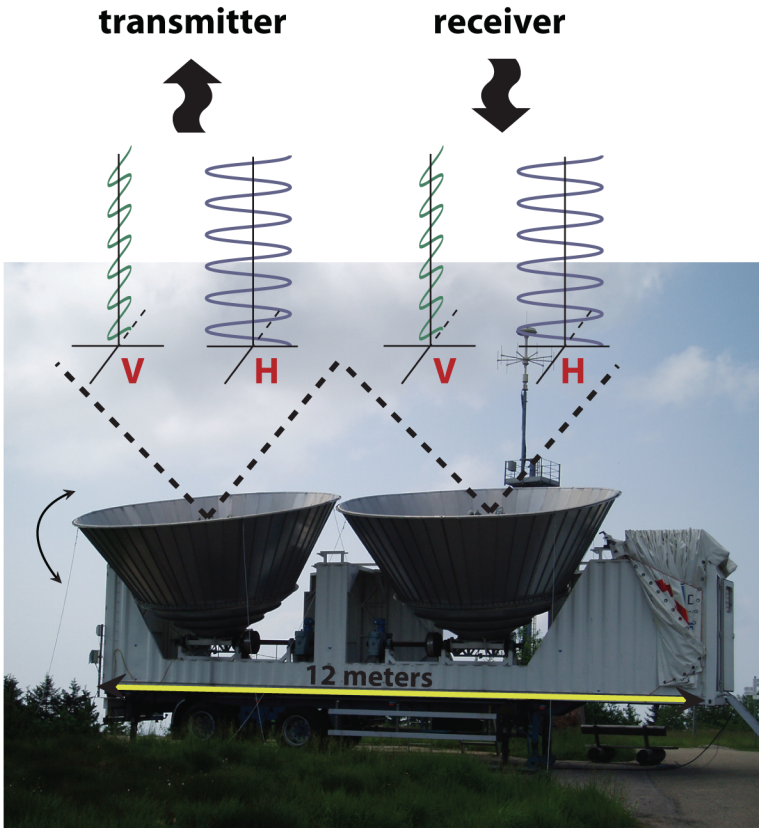

Fig. 1. The S-Band TARA radar. The transmitted and received signals are sequentially switched from vertical to horizontal polarization states in order to measure the full scattering matrix.

AMTD
4, 527–562, 2011

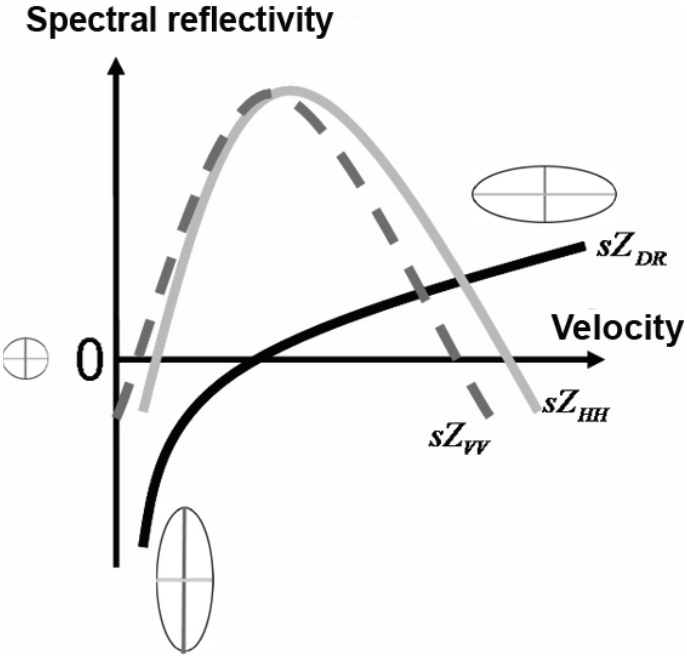

Fig. 2. Schematic representation of $sZ_{VV}(v)$, $sZ_{HH}(v)$ and $sZ_{DR}(v)$ and their relation to particle size and axis ratio.

AMTD
4, 527–562, 2011

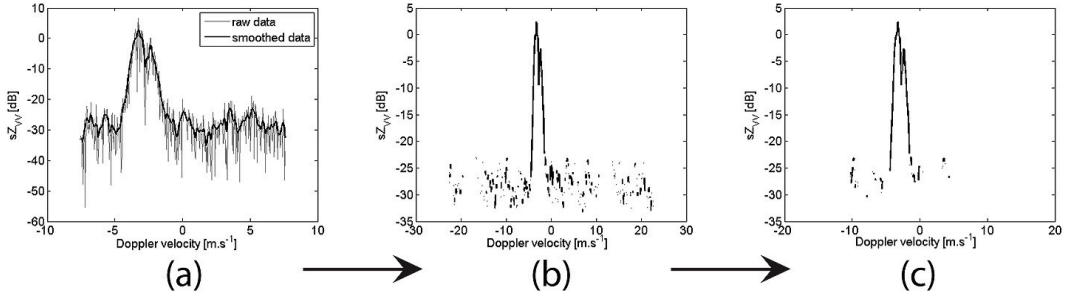

Fig. 3. TARA processing steps performed on $sZ_{VV}(v)$: **(a)** smoothing, **(b)** correction for spectra aliasing and non-simultaneous polarimetric measurements and **(c)** double $sL_{DR,x}$ clipping.

AMTD
4, 527–562, 2011

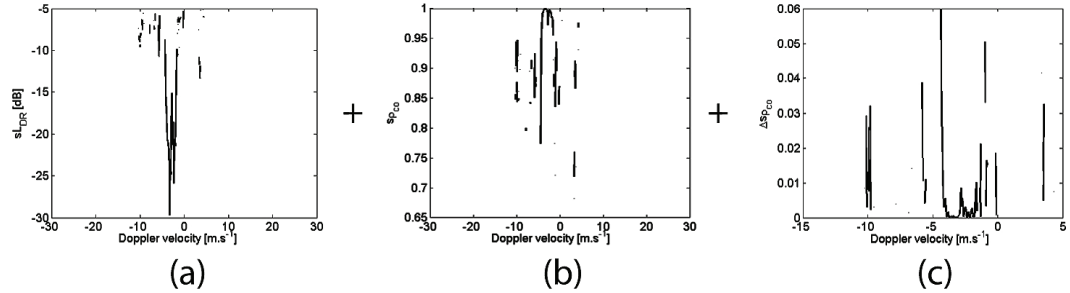

Fig. 4. Additional clipping performed on **(a)** $sL_{\mathrm{DR},v}(v)$, **(b)** $s\rho_{\mathrm{co}}(v)$ and **(c)** $\Delta s\rho_{\mathrm{co}}(v)$. This additional clipping gives the opportunity to constrain the Doppler velocity window (from $-3.8\,\mathrm{m\,s^{-1}}$ to $-2.7\,\mathrm{m\,s^{-1}}$ in this example).

AMTD
4, 527–562, 2011

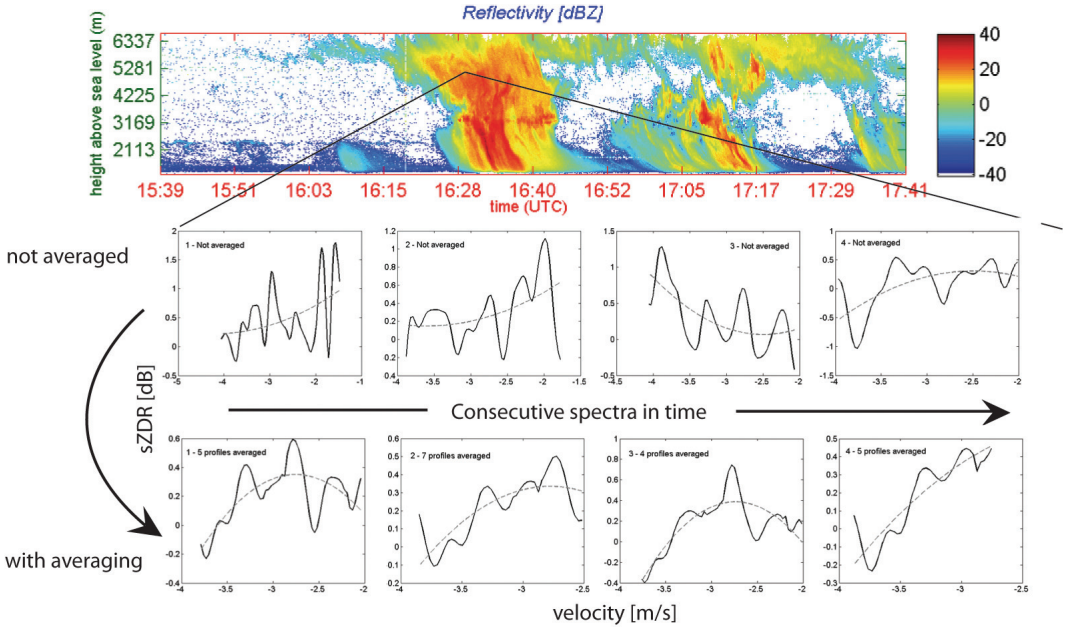

Fig. 5. Consecutive sZ_{DR} spectra extracted from an ice cloud region (see reflectivity profile). Each spectrum is measured at 1.5 s interval. The set of spectra are represented without (middle row) and with (bottom row) the additional averaging step. As displayed, the spectra become more coherent when the averaging is performed.

AMTD
4, 527–562, 2011

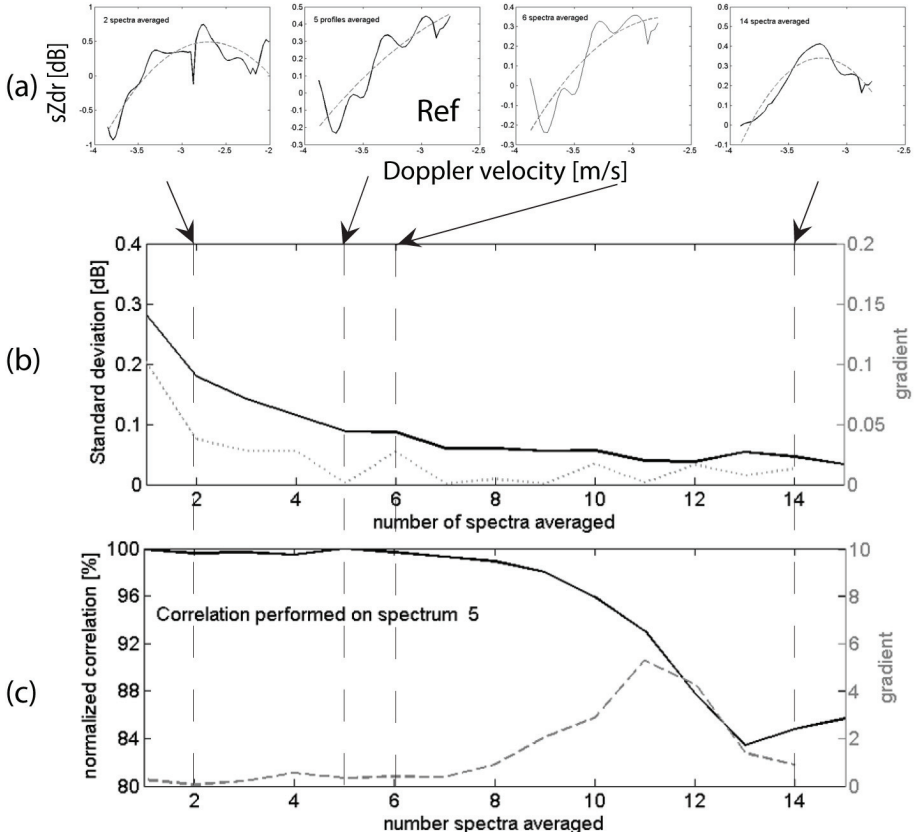

Fig. 6. Example of statistical analysis performed on sZ_{DR} parabolic fit for a specific time and range bin of a TARA measurement. **(a)** Representation of the sZ_{DR} spectra obtained with their polarimetric fit obtained for different number of spectra averaged (i.e. different averaging time). **(b)** Evolution of the standard deviation coefficient and its gradient obtained for each averaged spectra over an increasing spectral averaging time. **(c)** Evolution of the correlation coefficient R_d related to the averaged spectra number 5, where std is found below 0.15 dB.

AMTD
4, 527–562, 2011

Improvement of cloud microphysical retrievals

Y. Dufournet and H. W. J. Russchenberg

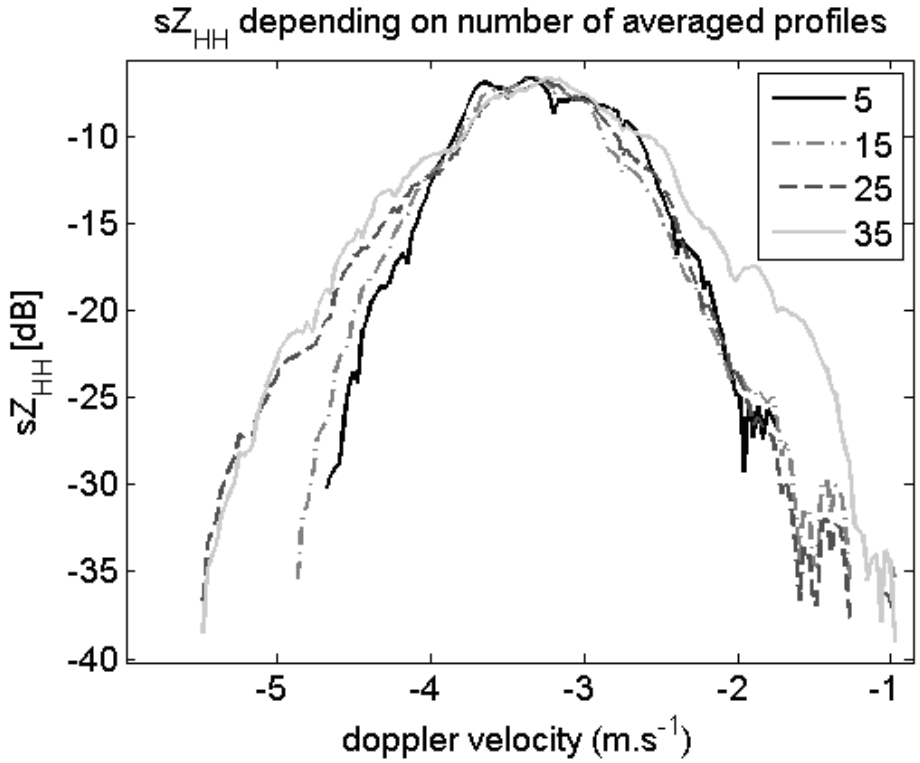

Fig. 7. Broadening effect observed on $sZ_{VV}(v)$ when an increasing number of initial spectra is averaged.

AMTD
4, 527–562, 2011

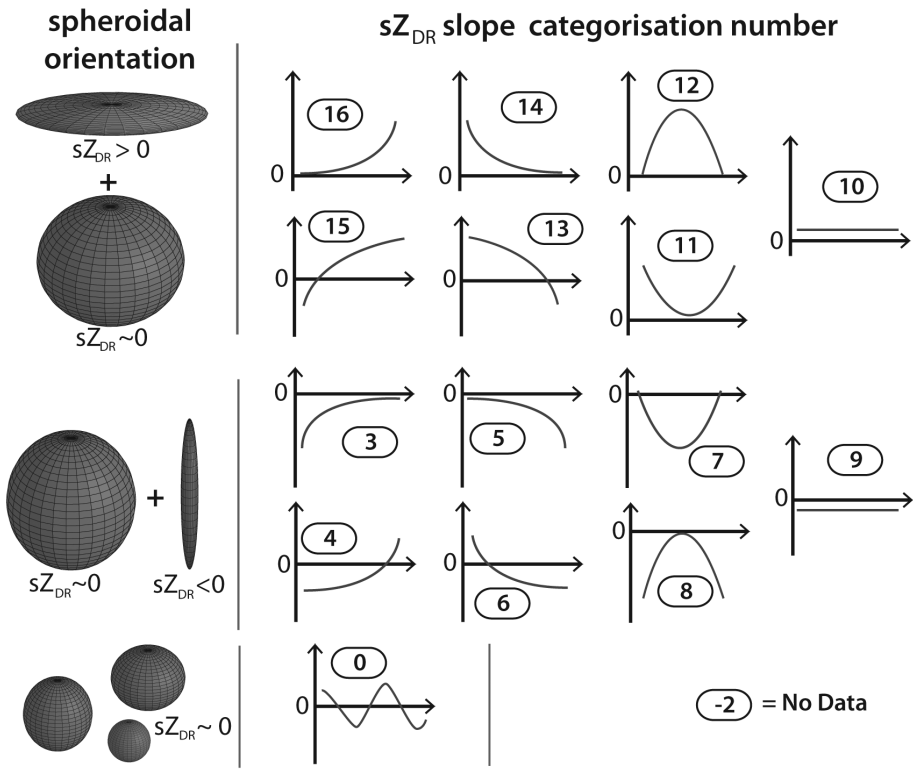

Fig. 8. sZ_{DR} classification based on the slope and values of the spectra. 16 different sZ_{DR} configurations have been sorted out from cloud observations. On the left hand side, a spheroidal representation of the assumed ice crystals shape(s) and orientation(s) is displayed depending on the sZ_{DR} configuration.

AMTD
4, 527–562, 2011

Fig. 9. Overview of the COPS domain. Each ground-based deployed during summer 2007 is represented in the picture (V = Vosges, P = Poldirad, H = Hornisgrinde, M = Murg valley – ARM site, S = Stuttgart) – 2009 Google.

AMTD
4, 527–562, 2011

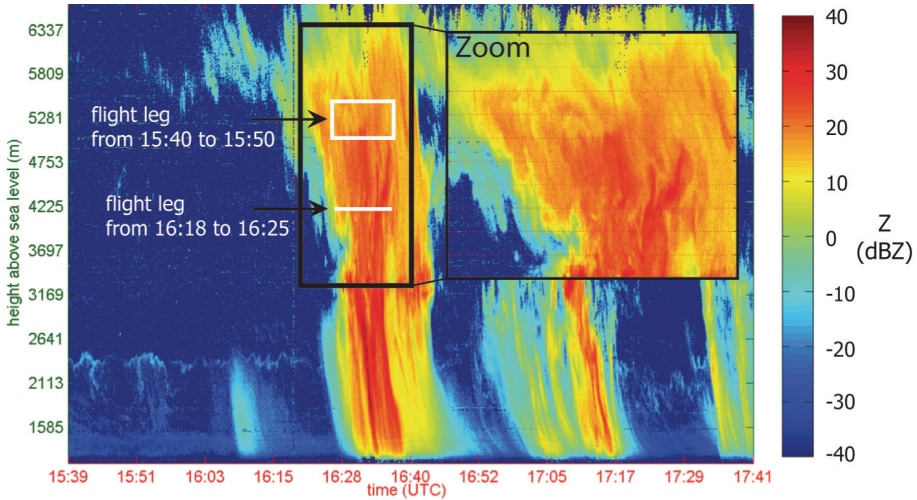

(a)

Fig. 10a. Microphysical results obtained from the TARA measurements on 21 July 2007. **(a)** Reflectivity profile from TARA. The black box delimits the boundaries of the area where the retrieval technique is applied. The white box represent the altitude of the flight legs performed by the ATR42 aircraft the same day. **(b)** Mapping of the categorization results. **(c)** Mapping of the weighting ratio R_w. **(d)** Histogram of L_{DR} values when R_w<2. **(e)** Simplified particle categorization obtained from **(b–d)**.

AMTD
4, 527–562, 2011

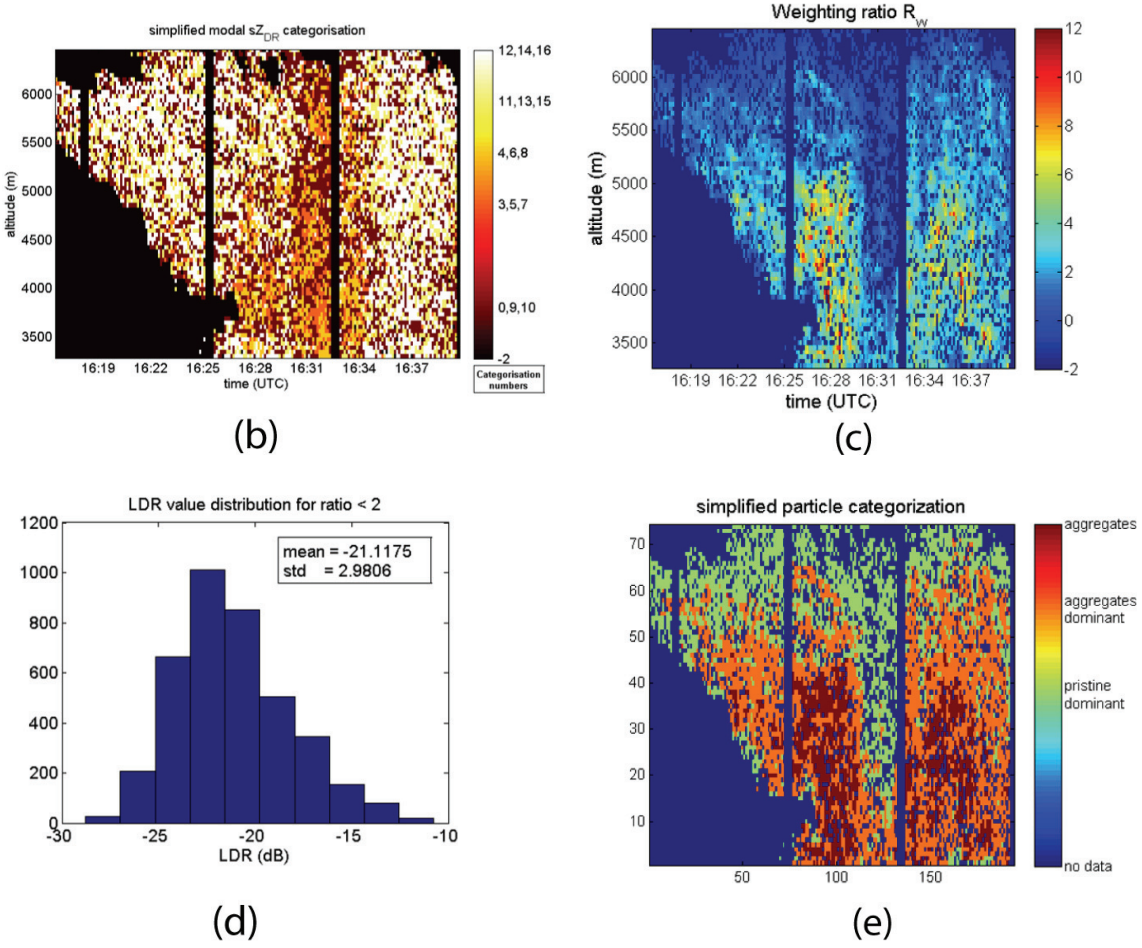

Fig. 10b. Continued.

AMTD
4, 527–562, 2011

Improvement of cloud microphysical retrievals

Y. Dufournet and H. W. J. Russchenberg

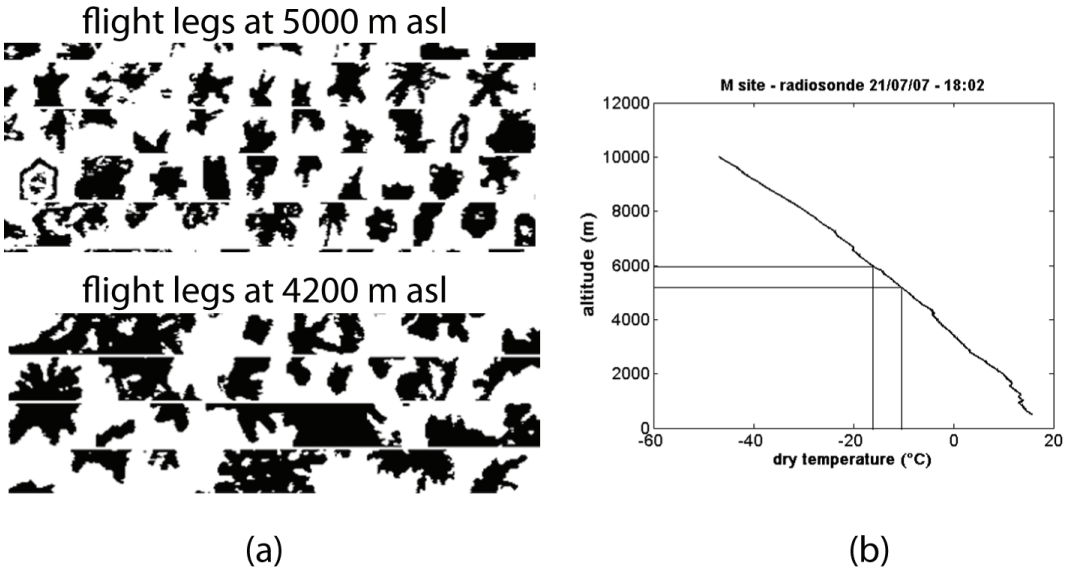

Fig. 11. Microphysical comparison with other sensors – **(a)** 2D-C probe images obtained from the ATR42 aricraft flying through the MCS event on 21 July 2007 at two different flight level. **(b)** Temperature profile obtained from a radiosonde launch on the M site also on 21 July 2007.

AMTD
4, 527–562, 2011